Geoderma 466 (2026) 117670

Contents lists available at ScienceDirect

Geoderma

journal homepage: www.elsevier.com/locate/geoderma

Dissolved organic matter dynamics and chemistry under fungal activity: A microcosm incubation with litter differentially ^{13}C-labelled

Thanh Thuy Nguyen Tu [a,*], Marion Texier [a], Rania Krimou [a], Philippe Biron [b], Sylvie Collin [a], Emmanuel Aubry [a], Mercedes Mendez-Millan [c], Christelle Anquetil [a], Caroline Kunz [d], Frédéric Delarue [a], Marie A. Alexis [a], Joëlle Dupont [e]

[a] Sorbonne Université, CNRS, EPHE, UMR 7619 METIS, F-75005 Paris, France
[b] Sorbonne Université, CNRS, IRD, INRAe, UPEC, Université Paris Cité, UMR 7618 iEES Paris F-75005 Paris, France
[c] Sorbonne Université, CNRS, IRD, MNHN, UMR 7159 LOCEAN, F-75005 Paris, France
[d] MNHN, CNRS, UMR 7245 MCAM, F-75005 Paris, France
[e] Sorbonne Université, CNRS, MNHN, EPHE, Université des Antilles, UMR 7205 ISYEB, F-75005 Paris, France

ARTICLE INFO

Handling Editor: Dr Daniel Said-Pullicino

Keywords:
Dissolved organic matter
Fungi
^{13}C-labelling
Chemical composition
Decomposition processes
Enzyme activity

ABSTRACT

This work aimed at better documenting the effects of fungal activity on dissolved organic matter (OM) in soils. Dynamics of water-extractable OM (as surrogate for dissolved OM) quantity and chemical quality was monitored during a ca. 6 month microcosm incubation of plant residues in the presence of fungi. Differential ^{13}C-labelling of metabolites vs structural compounds of the incubated residues further allowed clarifying the balance between fungal mineralisation and production of soluble compounds (through biosynthesis and/or decomposition). The fungus *Trichoderma harzianum* was mainly active during the first weeks of incubation, substantially mineralizing WEOM, preferentially consuming carbohydrates. The fungus induced chemical modification of WEOM, notably selective preservation of lipids and oxidation of lignin moieties. While *T. harzianum* probably degraded some insoluble structural molecules and produced biomass, these contributions to bulk WEOM appeared minor (when compared with leaching and mineralization), either because non-significant or entering non-extractable carbon pool. Additionally, characterization of control fungus-free microcosms, highlighted the potential role of abiotic processes on WEOM production, including leaching and depolymerisation by extracellular enzymes, notably of carbohydrate rich (insoluble) macromolecules.

1. Introduction

Soils correspond to the largest pool of terrestrial carbon as they comprise more carbon than atmosphere and global vegetation, combined (e.g. Eswaran et al., 1993; Lal, 2008). Although the primary source for organic carbon in soils is plant material, microorganisms are the actual builders of soil organic matter due to their constant metabolic activities (e.g. Kögel-Knabner, 2002; Liang et al., 2017). Microbial activity favours not only organic carbon recycling but also its inclusion in stable soil (micro)structures, under chemical forms of both high and weak preservation potential (Cotrufo et al., 2013; Lehmann and Kleber, 2015). Among soil microorganisms, fungi are the most efficient in degrading the lignocellulose complex of plant litters (Cooke and Rayner, 1984; Cragg et al. 2015) and fungal necromass contributes more to soil organic carbon than bacterial necromass (Nakas and Klein, 1979, Six et al., 2006, Li et al., 2022). Due to its high reactivity, dissolved organic matter (DOM) plays a crucial role in soils: it both constitutes a main carbon source for microorganisms and is an important contributor to sequestered carbon (e.g. Kalbitz et al., 2000; Lehmann and Kleber, 2015). The multiplicity and complexity of processes interplaying on DOM dynamics in soils has been integrated in the conceptual model built by Kalbitz et al. right from the beginning of this century: adsorption/-desorption from mineral (or organic) phases, leaching from plant and microbial biomass, mineralisation, assimilation and degradation by microorganisms, etc (Kalbitz et al., 2000). However, our knowledge on DOM and its dynamics still requires investigation, especially concerning the role of microorganisms and particularly fungi. Recent papers notably called for further studies on the balance between (1) carbon removal through mineralisation of DOM and (2) fungal contribution to DOM through biosynthesis or biodegradation of insoluble components into

* Corresponding author.
E-mail address: Thanh-thuy.Nguyen_tu@sorbonne-universite.fr (T.T. Nguyen Tu).

https://doi.org/10.1016/j.geoderma.2025.117670
Received 22 August 2025; Received in revised form 18 December 2025; Accepted 22 December 2025
Available online 20 January 2026

smaller ones (Liang et al., 2017; Gentile et al., 2024). Grassland ecosystems are ubiquitous in temperate and tropical areas; they constitute an essential pool for soil carbon sequestration, but are less studied than agricultural and forest soils (Jones and Donnelly, 2004; Bai and Cotrufo, 2022). The present work thus aimed at better documenting the effects of fungal activity on DOM dynamics in grassland soils.

A combination of microbiological and geochemical approaches were thus set up to document, among others, DOM chemistry at both bulk and molecular scales. Monitoring variations in DOM chemistry and sources through soil transformation may be complicated by the diversity of its components, whose chemical structure is often unspecific or non-diagnostic of microbial processes (Kelleher and Simpson, 2006; Kögel-Knabner, 2017). Differential ^{13}C-labelling of plant residues and their incubation allow tracing specifically carbon pools of different origin, notably metabolic and structural components (Girardin et al., 2009; Haddix et al., 2016). As a result, this study is based on a microcosm incubation of plant residues, differentially ^{13}C-labelled, in the presence of fungi. The experiment was achieved on leaf residues from a single plant species, *Lollium multiflorum* (Italian ray-grass), incubated by a single fungus, *Trichoderma harzianum,* so as to limit degrading trends due to variations in DOM source or microbial community, which may be difficult to identify. Ryegrass is among the most prevalent grass in natural and cultivated grasslands (Humphreys et al. 2010). *Trichoderma* corresponds to a cosmopolitan fungus in decaying woods, herbaceous litters and soils in general, thanks to its diverse metabolic capability including cellulose-, hemicellulose- and lignin-degrading enzymes (Gams and Bissett, 1998; Ahmed et al., 2009; Sharma et al., 2019; Bagewadi et al., 2017; Sánchez-Corzo et al., 2021). Water-extractable organic matter (WEOM), a common surrogate for DOM, was characterized by a multi-technique approach. Fungal enzymatic activity as well as elemental, isotopic and chemical composition of WEOM were monitored along a nearly 6-month incubation in order to evaluate the role of fungal activity on WEOM quantity and chemical quality. The strategy aimed at describing the transformation kinetics, as well as determining whether (1) specific WEOM compounds are preferentially mineralized and/or produced by the fungus and (2) *T. harzianum* substantially decompose insoluble macromolecular components into smaller extractable molecules.

2. Material and methods

The main experimental and analytical steps of the present study are synthesized as flowchart (Fig. 1).

2.1. Litter labelling

Plant residues were specifically ^{13}C-labelled to trace labile metabolites, taking advantage of the high turnover of metabolic carbohydrates that are continuously synthesized under a day-night regime (Girardin et al. 2009; Fahey et al. 2011). Growing mature plants under ^{13}C-enriched atmosphere for a few days before sampling enables strong labelling of metabolites to the contrary of storage compounds and structural polymers that are little sensitive to such short-term labelling. Italian ryegrass (*Lolium multiflorum* Lam.) was selected for its high leaf productivity and because it is widespread in temperate grasslands (Beckie and Jasieniuk, 2021). *L. multiflorum* seeds were sown in pots containing vermiculite, and plants grown for six weeks under natural atmosphere ($\delta\ ^{13}C_{CO2} \sim$ -8.8 ‰) in a controlled chamber with constant climatic conditions (SERVATHIN Rubic V, iEES Paris, Thiverval-Grignon, France; 70 % relative humidity, 400 ppmv CO_2, 23 °C day temperature, 12 h daylight period at 250 μmol/m^2/s of photosynthetically active radiation). Plants were fed twice a week with a Hoagland nutritive solution (pH 6). Three days before harvesting, ^{13}C-enriched CO_2 (+807.8 ‰) was continuously injected in the chamber from a bottle (10 % in abundance ^{13}C, Eurisotop) in mixing ratio of 1/10. CO_2 isotope composition (+808 ‰ in average) was monitored daily from purified

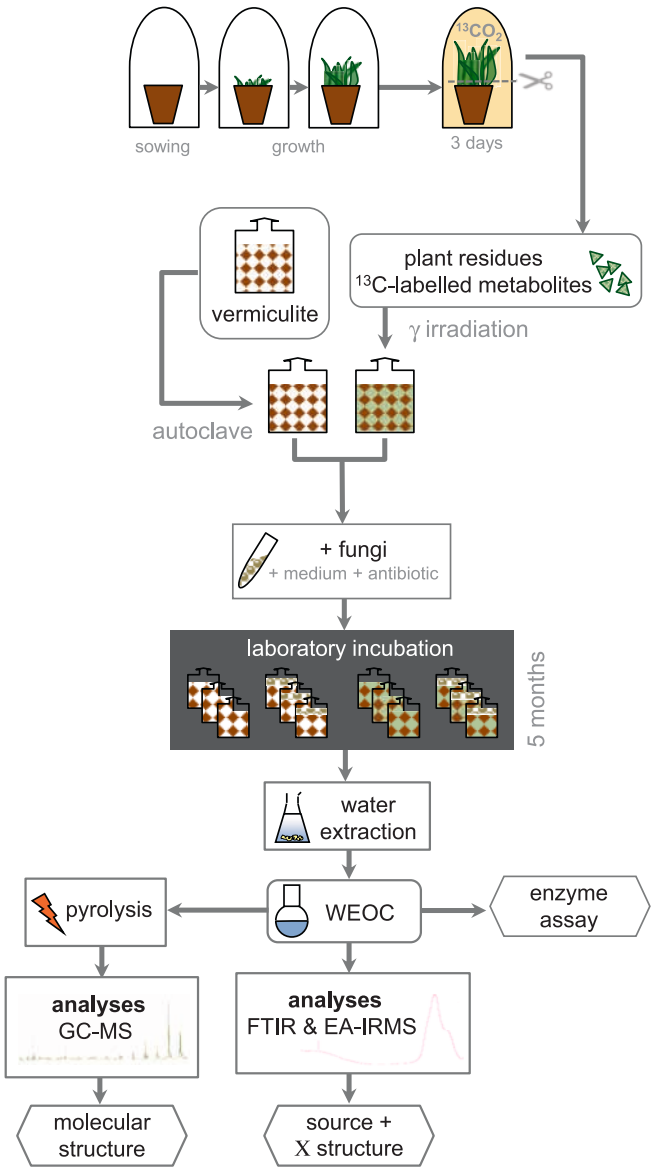

Fig. 1. Experimental protocol.

cryoscopic samples and measured with an isotope ratio mass spectrometer (Micromass/Elementar Dual Inlet).

At the end of the labelling period, ryegrass leaves were collected, dried to constant weight at 45 °C (ca. 3 days) and cut into pieces ca. 0.5 cm long which were thoroughly mixed for homogenisation. Bulk leaves composition was 36.5 %C, 4.5 %N with δ^{13}C + 115.1 ‰. The isotope composition of WEOM was + 246.4 ‰ while that of the extraction residue was + 65.4 ‰. Plant material was further sterilized by gamma irradiation (45–70 kGy, Ionisos, ISO14001, France) as this method was shown optimal for soil incubation studies (Maire et al., 2013).

2.2. Microcosm experiment

The experiment was performed in 250 ml glass bottles filled with ca. 7 g of vermiculite (millimetric pellets) and further autoclaved. 10 mL of Mandels medium (Mandels and Reese 1957) and 10 mL of antibiotic solution (teicoplanine, 200 μg/L final concentration) were added to each microcosm in order to favour the growth of the target fungus while inhibiting development of other microorganisms. About 2 g of γ-irradiated labelled plant material were added to the microcosms except the one used as control (i.e. containing no plant material). Half of the

microcosms were inoculated with 4 mL of water solution containing 14.10^6 spores of *Trichoderma harzianum* Rifai strain LCP3428 (MNHN, Paris, France), while 4 mL of autoclaved ultrapure water was added to the other half of the microcosms.

All in all, four treatments were applied to the microcosms: (1) no plant-no fungus, (2) no plant-fungus, (3) plant-no fungus and (4) plant-fungus. Bottle lids were left loose so as to allow gas exchange with atmosphere and microcosms of each treatment were incubated in separate chambers in the presence of CO_2 trap (1 M NaOH) to avoid cross contamination (CO_2 characterization was beyond the scope of this work). Incubation conditions were designed toward that of natural soils while promoting *T. harzianum* growth: 20 °C, 70 % relative humidity and 8 h daylight period (80 μmol/m^2/s of photosynthetically active radiation).

Microcosms were regularly watered (3 mL of autoclaved ultrapure water per month per microcosm) and examined with the naked eye for potential contamination by exogenous fungus. Microcosms exhibiting traces of development, even tenuous, of potential contamination by microorganisms other than *T. harzianum* were removed from the experimental design (3 out of 84 microcosms). Twice during the incubation (40 and 150 days), a few milligrams of randomly selected microcosms were taken for subculturing on potato dextrose agar and malt extract agar solid medium and further microscope examined so as to confirm the presence of *Trichoderma* fungus in the inoculated microcosms and the absence of any micro-organisms in the control microcosms. At the end of the incubation, DNA from 5 randomly selected subsamples were further sequenced for ITS1 and ITS2 molecular markers that confirmed identification with *T. harzianum*.

4 sets of triplicate microcosms were destructively sampled (i.e. sacrificed) at each of the seven time step investigated (1, 14, 28, 56, 91, 133 and 168 days), representing a total of 81 microcosms.

2.3. WEOM extraction

WEOM extraction protocol was adapted from Chantigny et al. (2007), after preliminary tests. The complete content of each microcosm was extracted with ultrapure water (1:50 w:w) for 2 h in a rotary shaker at 5 °C. Extracts were pre-filtered through nylon muslin (20 μm) and further centrifuged for 90 min at 5 °C and 5000 g. The supernatant was then filtered through nylon syringe filters (0.45 μm). Blanks and reference mixtures (vermiculite:unlabelled plants,7:2 w:w) were extracted along with each extraction batch for quality purposes. Aliquots of the obtained extracts were directly submitted to elemental analysis. Other aliquots were frozen at −20 °C in glycerol 20 % final concentration until determination of β −glucosidase activity. The remaining part of the extract was frozen at −20 °C, freeze-dried and crushed in a mortar prior to further analyses.

2.4. Chemical and isotope analyses

Raw data are available as supplementary materials (Table S1).

Dissolved organic carbon (DOC) and dissolved nitrogen (DN) were determined as non-purgeable organic carbon (NPOC) and total nitrogen (TN) using a TOC-L analyser (Shimadzu, Kyoto, Japan). C (TOC standard 25 mg.L^{-1}, Sigma-Aldrich, Saint Louis, Missouri, United States) and N (1 mg.L^{-1}N in H_2O, Merck Group, Darmstadt, Germany) standards were used as quantification references. Limits of detection and quantification were calculated based on the analysis of 10 extraction blanks: 0.14 mg.L^{-1} and 0.24 mg.L^{-1}, respectively, for NPOC, and 0.03 mg. L^{-1} and 0.07 mg.L^{-1}, respectively, for TN. DOC and DN contents were further normalized per gram of dry plant material (DPM) introduced in a given microcosm at the beginning of the experiment (mg.g^{-1}_{DPM}). WEOM C/N was calculated as weight ratio.

Approximately 0.2–0.3 mg of freeze-dried extracts were combusted using an elemental analyser (Thermo Fisher Scientific Flash, 2000) coupled to an isotope ratio mass spectrometer (Thermo Fisher Scientific Delta V advantage) to determine $\delta^{13}C$. Oak wood, tyrosine and urea were used as standards for isotopic calibration (standard deviation of ca. 0.1 ‰).

2.5. Enzyme assays

β-glucosidase enzymatic activity was measured according to Medina et al (2020) with minor modifications. The reaction mixture (0.5 mL) contained p-nitrophenyl- β −D-glucopyranoside (p-NPG, Sigma-Aldrich) as a substrate at a concentration of 2.4 mM in sodium citrate buffer 60 mM pH 4.8. Enzymatic activity was carried out in 1 mL spectrophotometer cuvettes. It was triggered by the addition of 100 μL of WEOM containing 20 % glycerol before the samples were immediately incubated at 30 °C, in triplicates. The reaction was stopped by the addition of 1 mL 2 M Ca_2CO_3 pH 11 and the amount of released p-nitrophenol (p-NP) was measured at 410 nm. Kinetics were carried out to calculate each activity after checking for linearity over a time period of 100 min. Calibration curves were established using p-NP (Sigma-Aldrich) solutions in reaction buffer (0, 25, 50, 100, 150, 200, 300 nmol). An absorbance of 1 corresponded to a variation of 83.8 nmoles. Activities were calculated using the following equation (Tab. S1):

$$V = [(\Delta A/min)x60x83.8x100]/8 \text{ in nmol/h.mL}$$

2.6. Infrared spectroscopy

Fourier transform infrared spectroscopy (FTIR) was performed with attenuated total reflectance (ATR) mode using a Bruker Tensor 27 spectrometer. The powdered lyophilised samples were placed directly on a germanium crystal. FTIR spectra were acquired by 64 scans at a 4 cm^{-1} resolution over the range 4000–600 cm^{-1}(Table S4). All spectra were corrected for water vapour, CO_2, baseline and for differences in depth of beam penetration at different wavelengths (ATR correction; Opus software). As the amount of each component, except plant residues and fungus, introduced in the bottles at the beginning of the experiment was identical in all microcosms, we hypothesized that the absorbance of their contribution to FTIR spectra is similar in all microcosms. Therefore, to eliminate contribution from vermiculite, antibiotic and Mandel medium, the mean spectrum of the WEOM obtained from the three control microcosms (no plant-no fungus) at initial time was calculated and subtracted from other spectra (Margenot et al. 2016).

2.7. Pyrolysis-GC-MS

Py-GC–MS analyses were carried out with a pyrolyzer (Pyroprobe 6250, CDS) coupled to a gas chromatograph (7890B, Agilent) and to a mass spectrometer (5977B, Agilent). Samples were pyrolyzed at 650 °C for 15 s under helium at 1 mL/mn. Tetramethylammonium hydroxide (TMAH 25 % methanol) was added as a derivatization agent in excess quantity. This thermochemolysis resulted in thermal cleavage concurrent with the chemical cleavage of ester and ether bonds of the OM, and simultaneously to the methylation of polar functional groups improving detection of these compounds. The released pyrolysis products were on-line separated using a non-polar GC column Rxi5Sil MS (30 m*0.25 mm*0.5 μm, Restek) through an oven ramp (initial temperature of 50 °C maintained during 10 min, raised at 2 °C/min until 320 °C, the final temperature, maintained during 13 min). The molecules were then ionized and fragmented in a mass spectrometer, working with an electron impact source (70 eV; 230 °C). Fragments were analysed with a simple quadrupole operating at 2 scans/s from 35 to 700 *m/z*. Each compound was identified based on literature and using the NIST library V2.3 (Table S5).

2.8. Statistics

Results are shown as means, error bars representing standard

deviations of the replicated microcosms for each treatment. When triplicate data were available, Student's t-tests were performed with XLStat-Pro (v2010 AddinSoft) to test for significant effect (p-value < 0.05) of fungus inoculation on biogeochemical features of WEOM on each time step (Table S2). Dynamics in element and isotope content of water extracts were further investigated fitting linear or exponential models in R statistical environment (R Development Core Team, 2015). Carbon and nitrogen content were modelled using linear models with day and fungus inoculation as independent variables. Stable carbon isotope composition fitted single exponential decay models $\delta\ ^{13}C_t = \alpha.e^{-kt} + \beta$, in which k is the constant rate (d^{-1}), and α and β isotope coefficients (‰) so that $\delta\ ^{13}C_0 = \alpha + \beta$ (Table S3). In the following sections, only differences which significance was statistically tested are described as significant.

2.9. Isotope mass balance calculation

Taking benefit of the differential ^{13}C-labelling, basic theoretical calculation of the isotope composition of bulk WEOM was achieved to test for potential (1) release, into WEOM, of OM from other fractions that are not water extractable and (2) uptake of some WEOM components into other carbon fractions (i.e. insoluble OM, CO_2, etc.).

The relative abundance and isotope composition of the various components of each carbon fraction cannot be determined from the present data, but as a first approach they were tentatively approximated to the basic mixture of two carbon pools: one dominated by relatively ^{13}C-depleted molecules (i.e. storage carbohydrates or structural polymers, 13D) and another one dominated by relatively ^{13}C-enriched molecules (i.e. metabolic carbohydrates, 13R) which relative amount is given by τ, so that the carbon content of a given carbon fraction CF can be written:

$C_{CF} = C_{13D} + C_{13R}$ with $C_{13D} = \tau^* C_{CF}$ and $C_{13R} = (1-\tau)^* C_{CF}$.

Considering one process P1 changing the carbon content of WEOM, the carbon released or uptaken (C_{P1}) can similarly be distributed into 13D and 13R so that $C_{P1} = C_{13D\text{-}P1} + C_{13R\text{-}P1}$

with $C_{13D-P1} = \tau_{P1}{}^* C_{P1}$ and $C_{13R-P1} = (1-\tau_{P1})^* C_{P1}$,

C_{P1} being positive or negative according to the process type.

After P1, the carbon content of WEOM at a given time step (*t*) can be written:

$C_{WEOM}(t) = C_{13D-WEOM}(t) + C_{13R-WEOM}(t)$

with $C_{13D\text{-}WEOM}(t) = C_{13D\text{-}WEOM}(t\text{-}1) + \tau_{P1}{}^* C_{P1}$ and

$C_{13R\text{-}WEOM}(t) = C_{13R\text{-}WEOM}(t\text{-}1) + (1\text{-}\tau_{P1})^* C_{P1}$; *t-1* corresponding to the time step preceding *t*.

The carbon released or uptaken from WEOM by additional processes may be similarly calculated. For example, with a second process P2 changing the carbon content of WEOM, the amount of the ^{13}C-depleted and ^{13}C-enriched pools car be determined with:

$C_{13D-WEOM}(t) = C_{13D-WEOM}(t-1) + \tau_{P1}{}^* C_{P1} + \tau_{P2}{}^* C_{P2}$ and

$C_{13R-WEOM}(t) = C_{13R-WEOM}(t-1) + (1-\tau_{P1})^* C_{P1} + (1-\tau_{P2})^* C_{P2}$

Supplementary processes may be further taken into account in the same way.

The isotope composition of a given carbon fraction corresponding to the weighted mean of the isotope composition of each of its pools, it can be expressed as $\delta_{CF} = [C_{13D}{}^* \delta_{13D} + C_{13R}{}^* \delta_{13R}]/C_{CF}$.

Considering as a first approach, that the isotope effects associated with degradation process(es) are small with respect to the labelled isotope compositions of the present study, the isotope composition of WEOM at a given time step can finally be expressed as:

$\delta_{WEOM}(t) = [C_{13D\text{-}WEOM}(t)^* \delta_{13D} + C_{13R\text{-}WEOM}(t)^* \delta_{13R}]/C_{WEOM}(t)$, with δ_{13D} and δ_{13R} being the isotope composition of the ^{13}C-depleted and ^{13}C enriched pools, respectively. $C_{13D\text{-}WEOM}$ and $C_{13R\text{-}WEOM}$ may be calculated with the above equations, according to the number of processes considered to change WEOM through degradation.

3. Results

3.1. Elemental contents

WEOM from microcosms incubated without plant material exhibited negligible carbon and nitrogen content (ca. 3.31 $mg.L^{-1}$ and 3.93 $mg.L^{-1}$, respectively) when compared with those containing plant organic matter (ca. 372.32 $mg.L^{-1}$ and 102.31 $mg.L^{-1}$, respectively). Their carbon and nitrogen contents remained stable throughout the incubation period and were similar in microcosms incubated with (3.34 $mg.L^{-1}$ and 3.32 $mg.L^{-1}$, respectively) and without (3.28 $mg.L^{-1}$ and 4.53 $mg.L^{-1}$, respectively) fungus (Table S1). As a result, *T. harzianum* did not develop in microcosms without plant material, and the C and N contribution from the spore inoculum, Mandels medium and antibiotics to WEOM was negligible. To enable comparison with literature and between microcosms with organic matter, DOC and DN contents were further normalized per gram of dry plant material introduced in a given microcosm at the beginning of the experiment.

WEOM of all microcosms containing plant organic matter exhibited a carbon content of ca. 62 $mg_{DOC}.g_{DPM}^{-1}$ at the beginning of the experiment, while reaching ca. 48 and ca. 121 $mg_{DOC}.g_{DPM}^{-1}$ at the end, in microcosms with and without fungus, respectively (Fig. 2). Carbon content from fungus-containing microcosms were significantly different from the fungus-free ones after 14, 28, 56 and 91 days of incubation ($p < 0.05$). WEOM from microcosms inoculated with fungus exhibited a sharp decrease in C during the first two weeks of incubation (−13 $mg_{DOC}.g_{DPM}^{-1}$) then remained stable, although this trend did not appear statistically significant. On the contrary, WEOM from microcosms without fungus showed a significant increase in carbon content through time ($p < 0.05$) for about 70 days before stabilizing around 110 $mg_{DOC}.g_{DPM}^{-1}$.

WEOM of all microcosms containing plant organic matter exhibited a nitrogen content of ca. 20 $mg_{DN}.g_{DPM}^{-1}$ at the beginning of the experiment, reaching ca. 14 and ca. 19 $mg_{DN}.g_{DPM}^{-1}$ at the end, in microcosms with and without fungus, respectively (Fig. 2). Nitrogen content from fungus-containing microcosms was significantly different from the fungus-free ones after 14, 28, 56 and 91 days of incubation ($p < 0.05$). Although more variable than carbon content, WEOM nitrogen content also tended toward higher values for microcosms without fungus when compared to those with fungus. While changes in nitrogen content of microcosms without fungus did not appear statistically significant, microcosms inoculated with fungus exhibited a significant decrease through time ($p < 0.05$). WEOM of microcosms containing plant organic matter exhibited a C/N ratio of ca. 3.0 at the beginning of the experiment, while it reached ca. 3.2 and ca. 5.7 after 24 week decay for microcosms with and without fungus, respectively (Fig. 2). C/N ratio differed significantly between both microcosm type ($p < 0.05$).

3.2. Isotope composition

In agreement with the negligible C contributions of the spore inoculum, Mandels medium and antibiotics to WEOM, at the beginning of the experiment, the microcosms containing only plant material had similar $\delta\ ^{13}C$ than the plant material itself: ca. 246 ‰. WEOM isotope composition followed exponential decays with constant rates significantly higher for microcosms with fungus than without fungus (Fig. 3, Table S3).

Theoretical isotope composition of bulk WEOM was calculated from mass balance as tentative estimation of the main processes potentially accounting for such decrease in isotope composition: (1) abiotic release of ^{13}C-depleted molecules from insoluble fraction, (2) fungal ingestion of ^{13}C-rich WEOM components and (3) release of ^{13}C-depleted compounds due to fungal degradation.

The carbon involved in these processes is approximated to the

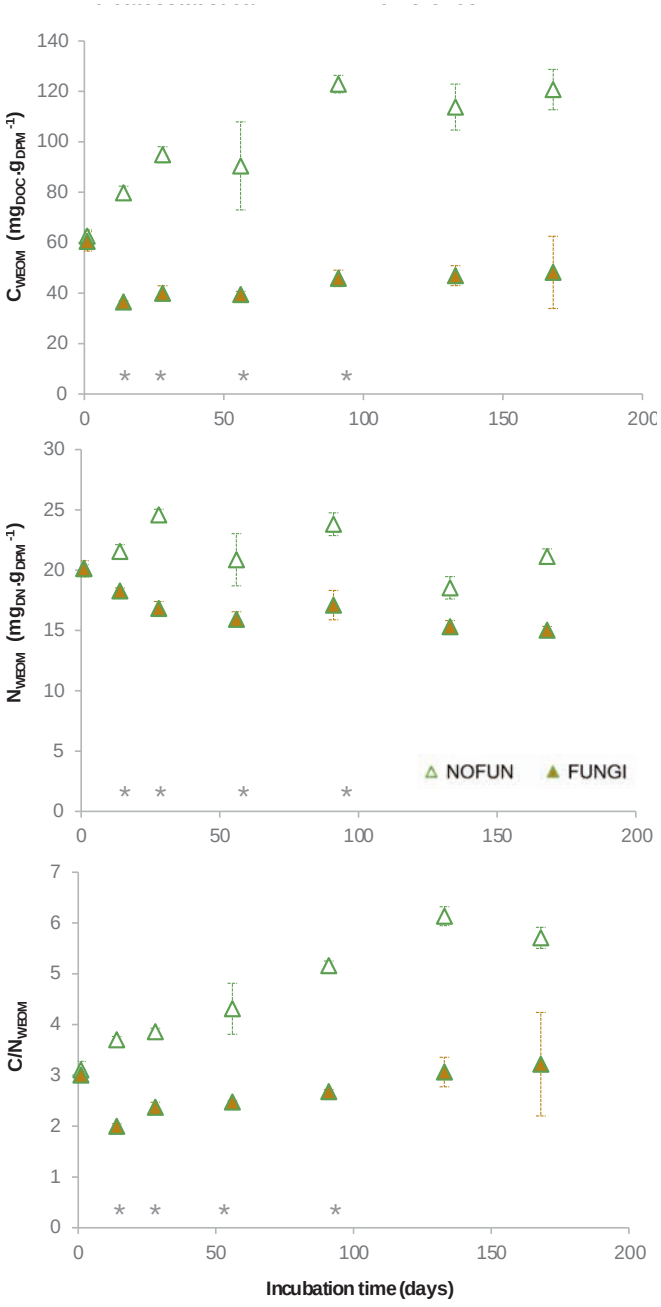

Fig. 2. Carbon and nitrogen content and C/N ratio of WEOM (mean ± SD) from microcosms incubated with (solid symbols) and without fungus (open symbols).* indicates statistically significant difference ($p < 0.05$).

mixture of a ^{13}C-depleted pool and a ^{13}C-enriched pool, in differing proportion according to the process considered (see experimental section 2.9). The amount of carbon provided by abiotic leaching was determined from the carbon content of microcosms without fungus (C_{NOFUN}) at two successive time steps (*t* and *t-1*): $C_{AB}(t) = C_{NOFUN}(t) - C_{NOFUN}(t-1)$. The amount of carbon removed by biomineralization was further calculated from the carbon content of microcosms with fungus (C_{FUNGI}) at two successive time steps and the carbon released by abiotic leaching, adjusted by a coefficient derived from the enzymatic activity of microcosms with fungus γ(t): $C_{BM}(t) = [C_{FUNGI}(t-1) + C_{AB}(t) - C_{FUNGI}(t)]^* \gamma$ (t). The carbon involved in each of these processes can further be divided into the ^{13}C-depleted pool and the ^{13}C-enriched pool, and the bulk isotope composition of WEOM calculated as the weighed mean of the combined ^{13}C-depleted pools and ^{13}C-enriched pools (see

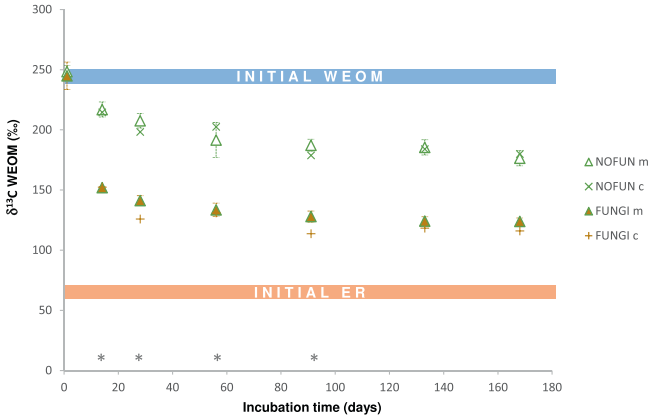

Fig. 3. WEOM isotope composition measured (m, triangles, mean ± SD) and calculated (c, crosses, mean) for microcosms incubated with (FUNGI) and without (NOFUN) fungus. Blue and red bands indicate the isotope composition of initial WEOM and extraction residue (ER), respectively; *: statistically significant difference ($p < 0.05$).

experimental section 2.9). Although several values can be applied within the frame of the initially measured bulk isotope values (+246 ‰ and + 65 ‰ for WEOM and extraction residue, respectively), calculation with abiotically leached carbon comprising 75 % of molecules relatively ^{13}C-depleted (~+50 ‰) and biomineralized carbon comprising 85 % of molecules relatively ^{13}C-enriched (~+300 ‰) is shown as a plausibility check on Fig. 3 (crosses). Tentative calculation adding a supplementary term to take into account the potential addition of biodegradation products of insoluble components (i.e. ^{13}C-depleted extraction residue) did not improve the results (data not shown).

3.3. β -glucosidase activity

Whether or not inoculated with *Trichoderma*, microcosms incubated without plant material exhibited, all along the experiment, enzymatic activity negligible (2.14 nmol/h.mL) when compared with those containing plant organic matter (between 22.95 and 195.93 nmol/h.mL according to time step and treatment; Table S1). Accordingly, the following is focused on microcosms incubated with plant litter.

A similar background level of activity was observed in both types of microcosms at time 0 day (Fig. 4). After 2 weeks, a 4-fold increase in the enzymatic activity was observed in the presence of *Trichoderma harzianum* but not when it was absent (significant difference, $p < 0.05$). After 29 days the activity had reduced and was similar to that observed at time

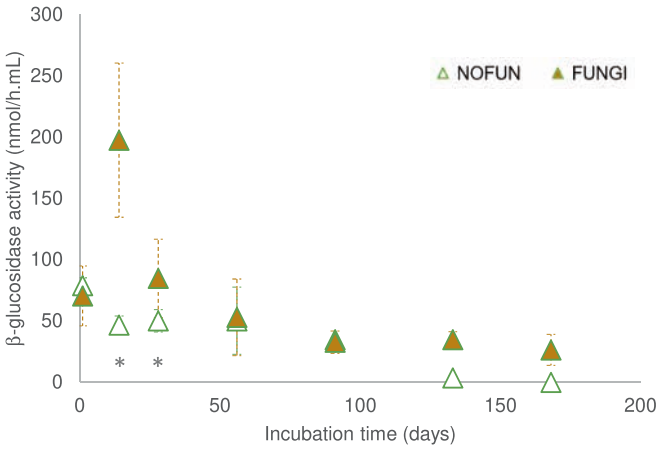

Fig. 4. β −Glucosidase activity of WEOM (mean ± SD) from microcosms incubated with (solid symbols) and without fungus (open symbols).

0 day in both conditions. In the following days, up the final sampling time, β −glucosidase activity remained at a background level in the fungus-containing microcosms, and went down to undetectable in the absence of the fungus.

3.4. Chemical analyses

WEOM chemistry was investigated by spectroscopy and spectrometry to further document the molecular changes associated with the elemental and isotopic changes described above. Although not suitable for (absolute) quantification, FTIR and Py-GC–MS can provide qualitative information on the chemical changes undergone by WEOM through incubation. Considering the negligible carbon content of the microcosms without plant material and the carbon dynamics evidenced, the following chemical study focuses on the microcosms incubated with plant material at initial time, after 28 days of incubation and final time (168 days).

The WEOM of all the microcosms containing plant material exhibited FTIR-ATR spectra typical for natural organic matter, with similar absorption bands indistinctive of the presence of fungus: a very broad band centred around 3200 cm^{-1} and three intense bands in the 1800–1000 cm^{-1} zone (Fig. 5). The 3200 cm^{-1} band is mainly attributed to the O-H bonds of residual water (He et al. 2009, Szymanski, 2017) likely trapped on the mineral and/or organic phase of the extract. The small band at ca. 2930 cm^{-1} is generally attributed to C-H bonds (Stevenson, 1982) but its smooth shape and inclusion with the shoulder of the previous band make it unsuitable to monitor the effects of incubation on WEOM

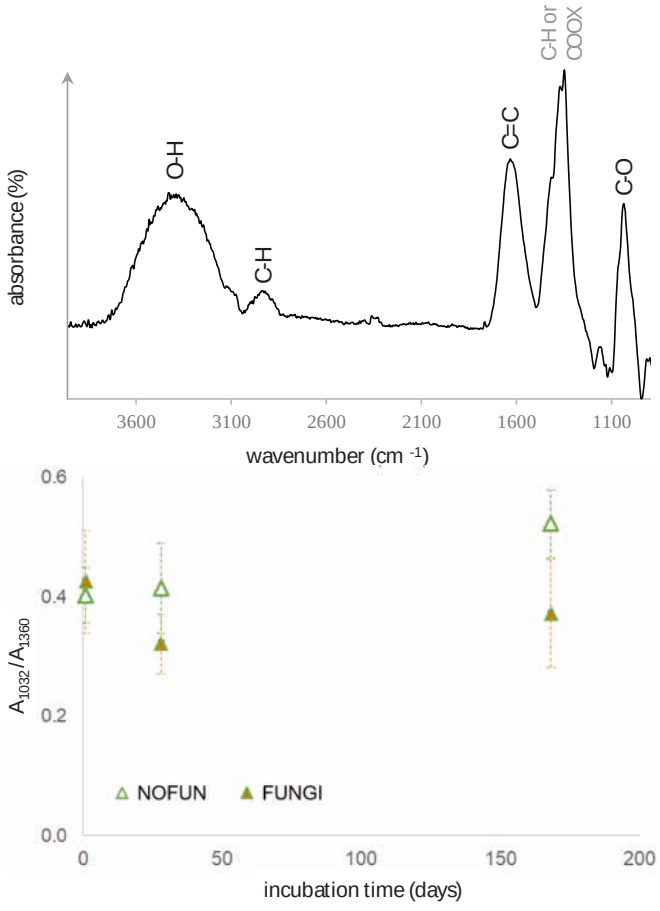

Fig. 5. FTIR-ATR characterization of samples: spectra typical of WEOM from microcosm incubated with plant material and fungi (168 days, top) and ratio of absorbance at 1350 cm^{-1} to 1032 cm^{-1} bands (mean ± SD, bottom) from microcosms incubated with (solid symbols) and without fungus (open symbols).

quality. The band maximizing at ca. 1612 cm^{-1} is generally attributed to aromatic C=C vibrations, symmetric stretching of COO^- groups, and H-bonded C=O of conjugated ketones (Stevenson, 1982; He et al., 2009, Szymanski, 2017). However, the lack of strong absorbance bands typical for the latter suggests the 1612 cm^{-1} band to be primarily attributed to aromatic C=C, probably mostly corresponding to lignin. The highest absorption band is centred around 1360 cm^{-1} and may be attributed to aliphatic C-H deformation and/or stretching of COO^- (Szymanski, 2017; Sharma et al., 2021). Finally, the band maximizing at ca. 1032 cm^{-1} was primarily attributed to C-O stretch of polysaccharides, according to previous soil studies on water extractable organic matter (Stevenson, 1982; Kalbitz et al., 1999; Szymanski, 2017).

WEOM of the studied microcosms appeared as a complex mixture of diversified components under py-GC–MS analyses (Fig. 6). The identified components correspond to molecules commonly reported in plant and soil, particulate and dissolved organic matter (Huang et al., 1998; Spencer et al., 2009; Wang et al., 2021a). These molecules can be classified into four main categories: phenolics, carbohydrate-derived compounds, nitrogen-containing molecules as well as aliphatics (Fig. 6). Most of the identified phenolic compounds comprise methoxy groups and various alkyl substitutions which are typical for lignin (Saiz-Jimenez and de Leeuw, 1986; Huang et al., 1998). No phenol exclusively originating from tannins could be detected. Basic phenols and benzene derivatives may also result from the pyrolysis of polysaccharides or proteins including fungal chitin (Chefetz et al., 2000; Saiz-Jimenez et al., 2021). Carbohydrate-derived compounds include various cyclic and acyclic (anhydro)-hexoses and −pentoses, including levoglucosan, the main pyrolysis product of cellulose (Pouwels et al., 1989; Shen and Gu, 2009). Most of the identified N-containing molecules correspond to typical pyrolysis products of amino acids (i.e. methylated derivatives, decarboxylation and/or cyclization products, Fig. 6) pointing to proteinaceous origin for these compounds (Stankiewicz et al., 1996; Templier et al., 2013). Although several of these compounds may originate from fungal chitin or melanin (e.g. pyridine- or pyrrolidine-containing molecules) in addition to plant proteins, none could be unambiguously attributed to fungi (Stankiewicz et al, 1996; Saiz-Jimenez et al., 2021). Identified aliphatic molecules mainly correspond to alkanes, acids and alcohols, saturated or not, some including further functionalized homologues (Fig. 6). While long chain aliphatics ($>C_{20}$) are typically of plant origin, the shorter one may equally be of plant or microbe origin (Eglinton and Hamilton, 1967; Wiensenberg et al., 2004).

4. Discussion

4.1. Abiotic release of WEOM

Increasing C-content and to a lesser extent N-content (Fig. 2), of WEOM from microcosms without fungus reveals substantial release and subsequent accumulation of soluble compounds, especially during the first weeks of incubation. All microcosms were sterilized at the beginning of the experiment, included teicoplanine antibiotic, and subculturing of fungus-free microcosms confirmed they remained sterile throughout the incubation period (see experimental section). Senescent leaves contain large amount of water-soluble molecules that are prone to physical leaching during (very) early decomposition (Benner et al, 1990; Maie et al. 2006; Nishimura et al. 2012). As a result, the observed WEOM release may be due to abiological processes. Although litter decomposition and DOC release were long thought as mainly controlled by microorganisms (e.g. Salamanca et al., 2003; Christ and David, 1996), abiological degradation of organic matter is now acknowledged as a significant process in soils (Kemmitt et al. 2008, Toosi et al. 2012; Zhou et al. 2020). It comprises mechanisms as diverse as solubilisation, chemical oxidation, chemical hydrolysis or else photodegradation (Austin and Vivanco, 2006; Toosi et al., 2014; Day et al., 2018; Wang et al., 2021b). The experimental conditions of the present incubation

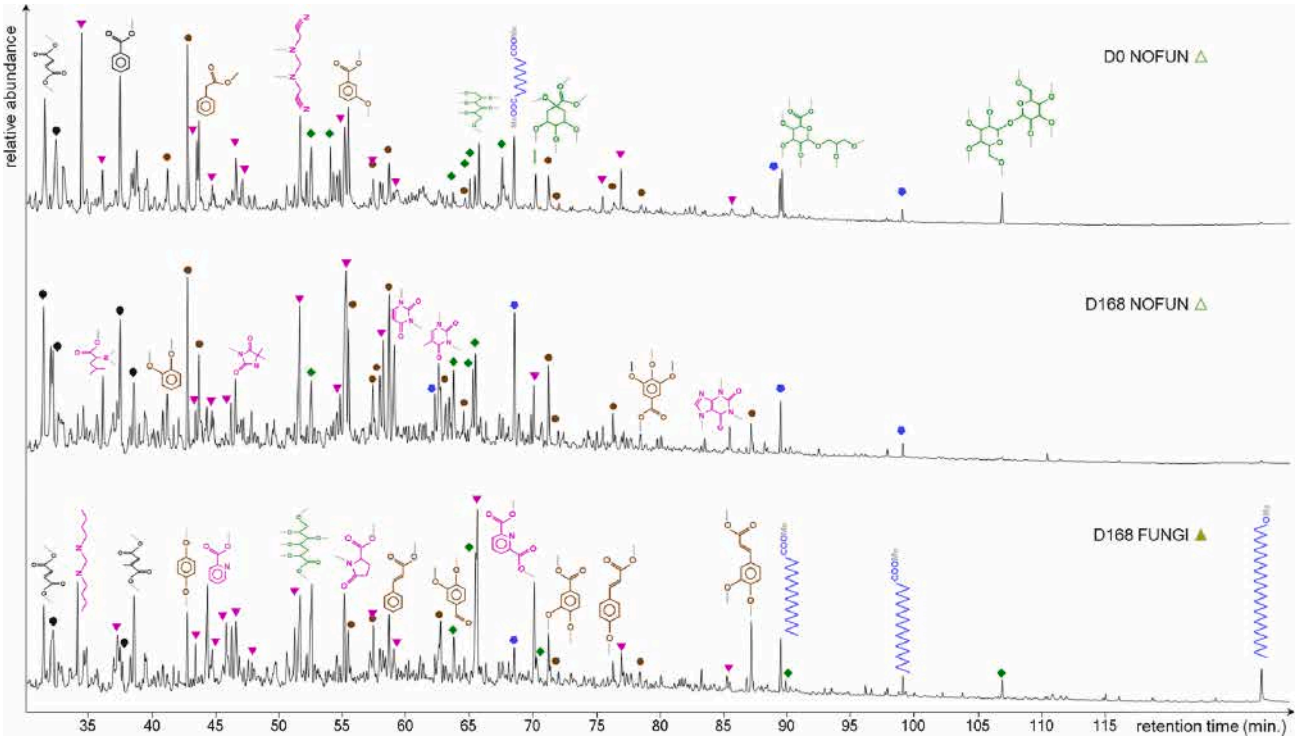

Fig. 6. 650 °C pyrochromatograms typical of WEOM from microcosms containing plant material at the beginning of the experiment (top, without fungi), and after 168 day-incubation without (middle) and with (bottom) fungus. Brown molecules and discs: lignin derivatives, green molecules and diamonds: carbohydrates, pink molecules and triangles: N-containing compounds, blue pentagons and molecules: aliphatics, black symbols correspond to ubiquitous compounds. Most compounds occur in the three pyrochromatograms so that molecular structures were shown alternatively in one of the three, so as to limit graphic overload.

(regular watering, light–dark cycles, …) are compatible with such mechanisms. The metabolism associated with the residual enzymes naturally present in soils is also often included in abiotic degradation processes (Maire et al., 2013; Kéraval et al. 2016; Lohse et al., 2022). These enzymes may correspond to those excreted by soil microorganisms or those naturally included in plant residues (either extracellular or intracellular); such enzymes are generally preserved in soils thanks to associations with minerals or plant or microbial necromass. In the present study, such enzymes most likely originate from plant residues as no activity could be detected for the microcosms incubated without plant residues. Non-zero value of β −glucosidase activity in fungus-free microcosms, notably at the beginning of the experiment, shows this enzyme remained active in spite of gamma ray sterilisation of plant residue, and further suggests abiotic enzymatic activities for our *in vitro* experiment. Subsequent accumulation of released compounds is to relate with the *de facto* absence of microbial mineralization.

Although the cation exchange capacity of vermiculite is rather high, its potential to adsorb dissolved organic matter is negligible excepted when modified by cation exchange or intercalation (Abate et al. 2006). As a result, the marked increase in WEOM carbon content without fungus also suggests that potential adsorption of WEOM on the vermiculite pellet remains probably constant during incubation and minor with respect to litter decomposition processes. Increasing WEOM C/N ratio (Fig. 2) further suggests that these abiotically released molecules are N-depleted and qualitative chemical ratios (Figs. 5 & 7) point to substantial contribution of carbohydrate to the released and accumulated products. Carbohydrates are indeed recognized as main components of soluble litter material that are notably released during (very) early degradation (Benner et al. 1990, Kalbitz et al., 2003; Hishi et al. 2004). WEOM isotope composition (Fig. 3) decreases toward that of extraction residue of undegraded plant material, further suggesting abiotic release-degradation of linked (or polymerised) material. Although these early degradation patterns are in agreement with literature (Osono and Takeda, 2001; Kalbitz et al. 2003; Zhu et al., 2022a,b), the present study highlights the potential role of abiotic processes in OM degradation.

4.2. Early fungal activity

As incubation proceeds, carbon, C/N and to a lesser extent nitrogen content of WEOM from microcosms inoculated with *T. harzianum* showed trends different from those without the fungus, pointing to fungal activity, especially during the first month of the experiment (Figs. 2 and 4). Higher β −glucosidase activity in the fungus-inoculated microcosms when compared with the others further confirms *T. harzianum* activity. β −glucosidase (β −D-glucoside glucohydrolase, EC 3.2.1.21) belongs to the glucosidase class that catalyze the hydrolysis of 1–4 β −glucosidic linkages of aryl-, amino- or alkyl- β −glucosides, β −linked oligosaccharides and other oligosaccharides, finally releasing D-glucose. In fungi they are part of the cellulosome and are involved in the last step of cellulose degradation by degrading cellobiose to D-glucose. In several *Trichoderma* species, β −glucosidase has been found in association with cell wall and/or purified from the extracellular medium (Tiwari et al 2013). *T. harzianum* is actually among the first fungi to colonize decomposing leaves in the succession of soil decomposers (Osono & Takeda, 2001). In agreement with literature on soil and compost WEOM, elemental contents decrease, as a result of microbial mineralization (Christ and David, 1996; Hishi et al., 2004; Said-Pullicino et al., 2007; Bahadori et al., 2021). Decrease in WEOM carbon content toward 3/4 of the initial value after one month (Fig. 2) indicates *T. harzianum* not only consumes the carbon released by abiotic degradation, but also a significant part of the WEOM initially present in plant material.

The WEOM from the present study appeared, upon chemical and molecular analyses, as a complex mixture of carbohydrates, lignin, protein and lipid derived compounds (Figs. 5 and 6), in agreement with previous studies on soil OM (Huang et al., 1998; Wang et al., 2021a). At first sight, the relatively high diversity and relative abundance of

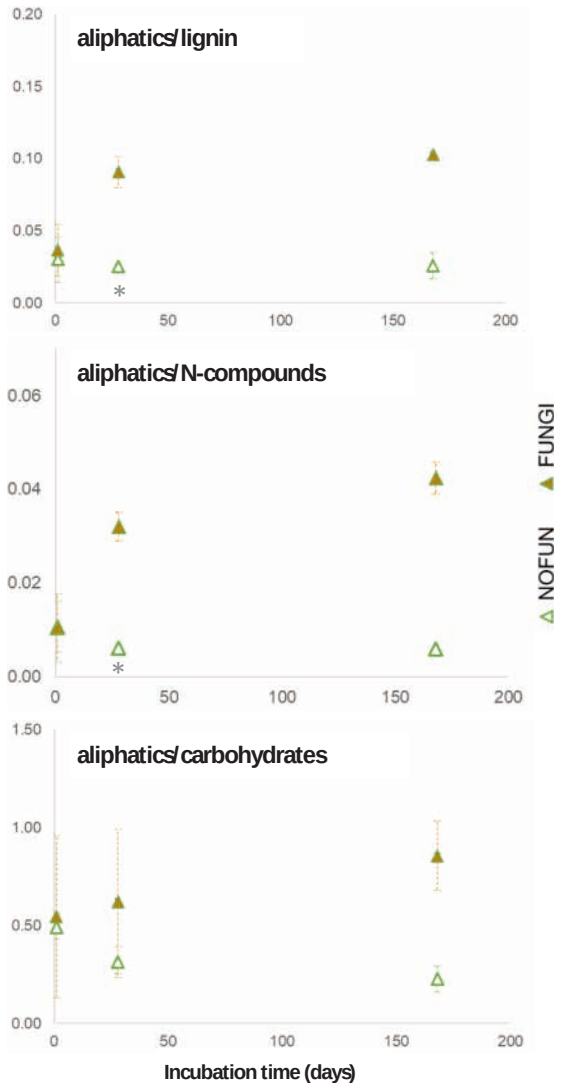

Fig. 7. Abundance ratios of the main compound families identified by Py-GC-MS analyses of WEOM (mean ± SD) from microcosms incubated with (solid symbols) and without fungus (open symbols). The relative abundance of each compound family was derived from pyrochromatogram peak areas (i.e. sum of all the identified compounds of the family); * indicates statistically significant difference ($p < 0.05$).

carbohydrate derived- and N-containing compounds suggested only slightly degraded OM as these compounds are generally considered as relatively sensitive to degradation (Opsahl and Benner, 1995; Mikutta et al., 2006). While FTIR-ATR spectra show no obvious trend through incubation, a slight decrease in the ratio of absorbance at 1032 cm^{-1} to that at 1360 cm^{-1} for microcosms with fungus when compared the fungus-free one can be noted. As a result, *T. harzianum* may have induced an apparent preferential degradation of polysaccharides when compared with other components (Fig. 5), first consuming easily degradable plant material such as carbohydrates for its metabolism.

No unambiguous fungal biomarker could be detected in substantial amounts in the pyrolysates of the WEOM extracted from microcosms inoculated with *T. harzianum*. Aside from ω–OH fatty acids, ergosterol and, to a lower extant, 3-acetamidopyrones, that are recognized as markers of fungal biomass but were not detected here, most pyrolysis products associated with fungi or fungal decay of plant organic matter can also correspond to plant or unspecific soil organic matter components. Indeed, the cracking of (macro)molecules during pyrolysis and the potential rearrangement of the obtained moieties, often lead to unspecific compounds (Sobeih et al. 2008). As a result, small fungal production may have remained undetected here. While pyrochromatograms show no obvious trend through incubation (Fig. 6), abundance ratios of main compound families tend to exhibit different kinetics according to the presence of the fungus (Fig. 7, Tab. S1). N-compounds, carbohydrates- and lignin-derived molecules exhibit no particular trend with respect to each other through incubation, but seem preferentially degraded when compared with aliphatics in the presence of *T. harzianum* (Fig. 7). This is in agreement with the often assumed high preservation potential of lipids (Opsahl and Benner, 1995; Zonneveld et al., 2010) and the possible production of water soluble aliphatics during fungal degradation (of lignin; Khatami et al., 2019).

The absence of a noticeable relative degradation trend in pyrochromatograms between carbohydrates, lignin moieties and nitrogen-containing compounds is to relate to the fact that soluble organic matter is not only a substrate for fungal growth and activity, but may also include products of microbial metabolism. The contribution of microbial carbohydrates, peptides and even free fatty acids to WEOM was indeed evidenced in several soil and compost studies (Kalbitz et al., 2003; Haynes, 2005; Said-Pullicino et al., 2007). Although tenuous, the slight carbon increase from 2 months of incubation (Fig. 2) may further support the hypothesis of fungal production of WEOM compounds. Considering the relative chemical stability of aromatic compounds, accumulation of lignin-derived products may be expected in WEOM as incubation proceeds (Kalbitz et al., 2003; Said-Pullicino et al., 2007). This was not the case here, suggesting actual degradation of this macromolecule (and/or its soluble derived products). Fungal degradation of lignin is further confirmed by qualitative changes among lignin derived compounds: guaiacyl- and *p*-coumaryl moieties appear preferentially degraded with respect to syringyl-moities that additionally exhibit a marked increase in acid/aldehyde ratio (Fig. 8). Indeed, an increase in the acid/aldehyde ratio of syringyl phenols is typical for lignin oxidation (Goñi et al., 1993; Robertson et al., 2008; Nakakuni et al., 2023). Syringyl moieties are generally preferentially degraded during early degradation of soil OM or isolated lignin (Ziegler et al., 1986; Huang et al., 1998; Pichler and Kogel-Knabner, 2000); their relative enrichment in WEOM may suggest (1) lignin degradation mechanisms are different for *T. harzianum* from that of previously documented microorganisms, and/or (2) contribution from insoluble OM (that is biodegraded into smaller molecules extractable with water).

Inoculated microcosms seem to attain an apparent steady-state after a few weeks (Figs. 2-4), probably due to *T. harzianum* starvation as soon as easily metabolisable carbohydrates and nitrogen are no longer available, in agreement with previous *in vitro* studies on the decomposition of DOM or humic substances by fungi (e.g. Lerch et al., 2011; Collado et al., 2018; Gentile et al., 2024).

4.3. Fungal decay of insoluble compounds?

While (bio)chemical patterns undoubtedly point to fungal consumption of WEOM, indicators of degradation of insoluble OM into WEOM components are rather tenuous: slight carbon increase from 2 months of incubation, relative increase in aliphatics when compared with other compound families, relative changes in the chemistry of lignin moieties. Isotope patterns of incubated microcosms were thus further investigated to test whether *T. harzianum* actually degraded insoluble OM, taking advantage of the differential ^{13}C-labelling of plant residues.

Both abiotic release of WEOM and fungal activity lead to a decrease in WEOM isotope composition, this ^{13}C-depletion being significantly higher in the presence of *T. harzianum* (Fig. 3). Although fungal activity had clearly a significant impact on WEOM ^{13}C-content, several isotope processes should be taken into account for both microcosm types. Chemical bonds involving heavy isotopes being harder to break and build, kinetic isotope effect associated with OM degradation and biosynthesis generally favours the production of ^{13}C-depleted molecules

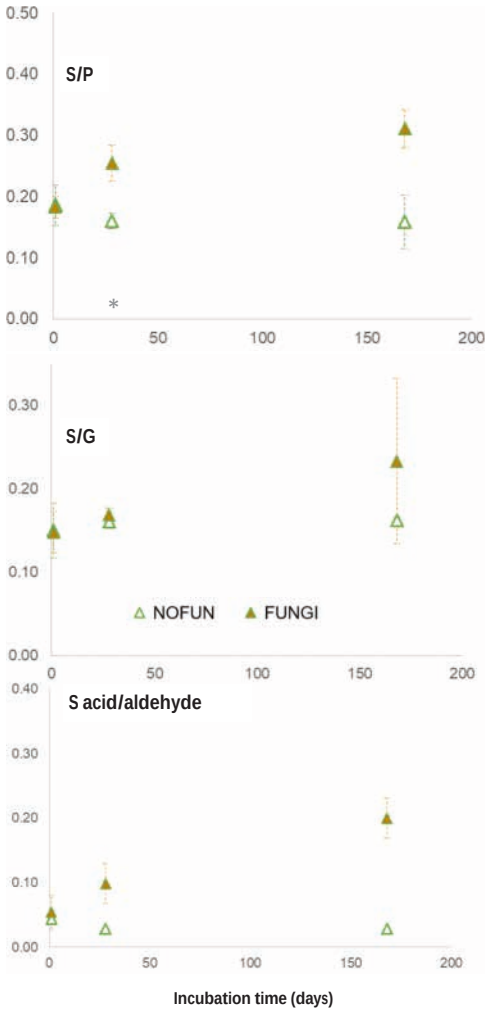

Fig. 8. Lignin degradation ratios of WEOM (mean ± SD) from microcosms incubated with (solid symbols) and without fungus (open symbols). The relative abundance of each compound family was derived from pyrochromatogram peak areas (i.e. sum of all the identified compounds of the family); * indicates statistically significant difference ($p < 0.05$).

(Urey, 1947; Fry, 2006). Yet, these kinetic isotope effects are small (i.e. no more than a few per mil; Blair et al., 1985; Ghashghaie et al., 2003; Tcherkez, 2010; Lerch et al., 2011) when compared with the measured changes. Accordingly, they likely only played a minor role on the isotope signature of the studied WEOM. The observed isotope patterns more likely reflect relative changes in the different carbon pools contributing to WEOM. The three days isotope labelling applied to the plants led to contrasted isotope composition of WEOM and extraction residue (246 ‰ and 65 ‰, respectively), each being likely composed of molecules of different isotope composition as a consequence of their various multi-step biosynthetic pathways (Girardin et al., 2009; Haddix et al., 2016).

WEOM may thus have undergone isotope variation due to preferential uptake and/or addition of carbon from pools of isotope composition differing from initial WEOM. The processes the most likely involved are (1) abiotic leaching of ^{13}C-depleted molecules released from insoluble fraction, (2) fungal consumption of ^{13}C-rich WEOM components and (3) release of ^{13}C-depleted molecules upon fungal degradation. Theoretical isotope composition of bulk WEOM was calculated from mass balance as tentative estimation of these processes (see result section 3.2). Calculated isotope compositions only considering the two first processes are in rather good agreement with the measured values (Fig. 3). Tentative calculation adding a supplementary term to take into account the potential addition of biodegradation products of insoluble components did not improve the results (data not shown) so that this process may have played a minor role on bulk WEOM.

As a result, abiotic release of ^{13}C-depleted carbon from insoluble OM combined to preferential biomineralization of ^{13}C-rich carbohydrate of WEOM probably constitute the main processes controlling the observed degradation patterns. Although (1) isotope fractionation undoubtedly occurred, and (2) some chemical pattern suggested biodegradation products of insoluble OM and fungal biomass may have contributed to WEOM, these processes probably only played a minor role in the present experiment.

5. Conclusion

This ca. 6 months monitoring of litter-vermiculite microcosms first allowed highlighting the potential role of abiotic processes on WEOM production, including leaching and depolymerisation by extracellular enzymes, notably of carbohydrate rich (insoluble) macromolecules. The fungus *T. harzianum* was mainly active during the first weeks of incubation, mineralizing not only abiotically released but also initial WEOM, preferentially consuming carbohydrates. The chemical modification of WEOM induced by this fungus also implied selective preservation of lipids and oxidation of lignin moieties. While *T. harzianum* probably degraded some insoluble structural molecules and produced biomass, these contributions to bulk WEOM appeared minor (when compared with leaching and mineralization), either because non-significant or entering non-extractable carbon pool. As a result, the studied fungus probably mainly played a catabolic rather than anabolic role on this soil OM pool (Liang et al., 2017). The modifications of WEOM induced by this single fungus are substantial but limited in time. Further experiments taking into account the complexity of soils, especially the succession of the diverse microbial populations naturally occurring in soils are now necessary to try to extrapolate the present results to natural soils.

CRediT authorship contribution statement

Thanh Thuy Nguyen Tu: Writing – review & editing, Writing – original draft, Supervision, Project administration, Methodology, Investigation, Funding acquisition, Conceptualization. **Marion Texier:** Writing – review & editing, Investigation. **Rania Krimou:** Investigation. **Philippe Biron:** Writing – review & editing, Investigation. **Sylvie Collin:** Writing – original draft, Supervision, Methodology, Investigation. **Emmanuel Aubry:** Investigation. **Mercedes Mendez-Millan:** Writing – review & editing, Supervision, Methodology, Investigation. **Christelle Anquetil:** Writing – review & editing, Methodology, Investigation. **Caroline Kunz:** Investigation. **Frédéric Delarue:** Writing – review & editing, Methodology. **Marie A. Alexis:** Writing – review & editing, Methodology, Investigation. **Joëlle Dupont:** Resources, Methodology, Conceptualization.

Declaration of competing interest

The authors declare that they have no known competing financial interests or personal relationships that could have appeared to influence the work reported in this paper.

Acknowledgements

We are indebted to Thierry Bariac for access to the controlled chamber and to Patricia Richard for technical and analytical support during the labelling experiment. Thanks are also due to Sandrine Lacoste and Gail Monvoisin for taking care of *Trichoderma* cultures. We are grateful to Sylvain Théry and Bénédicte Sabatier for assistance on preliminary experiments during COVID lockdown. We also thank Aliénor Allain and Katell Quénéa for valuable help in interpreting IR and SM

data, respectively. We are grateful to Laurent Rémusat, Delphine Derrien, Thomas Lerch and Julie Leloup for smart advices on experimental design. Helpful discussions with Sylvie Derenne, Nicolas Valette, Maryse Rouelle, Pierpaolo Zuddas and Arnaud Huguet deserve warm acknowledgements as well. Isotopic analyses were performed at the ALYSES platform (IRD/SU, Bondy) and statistical modelling were run by LEKIRO. This work was funded by a grant from CNRS-INSU (EC2CO AO2019) which was greatly appreciated

Appendix A. Supplementary data

Supplementary data to this article can be found online at https://doi.org/10.1016/j.geoderma.2025.117670.

Data availability

Data will be made available on request.

References

Abate, G., dos Santos, L.B., Colombo, S.M., Masini, J.C., 2006. Removal of fulvic acid from aqueous media by adsorption onto modified vermiculite. Appl. Clay Sci. 32 (3–4), 261–270.
Ahmed, S., Bashir, A., Saleem, H., Saadia, M., Jamil, A., 2009. Production and purification of cellulose-degrading enzymes from a filamentous fungus Trichoderma harzianum. Pak. J. Bot. 41 (3), 1411–1419.
Austin, A.T., Vivanco, L., 2006. Plant litter decomposition in a semi-arid ecosystem controlled by photodegradation. Nature 442, 555–558.
Bagewadi, Z.K., Mulla, S.I., Ninnekar, H.Z., 2017. Purification and immobilization of laccase from Trichoderma harzianum strain HZN10 and its application in dye decolorization. J. Genet. Eng. Biotechnol. 15 (1), 139–150.
Bahadori, M., Chen, C., Lewis, S., Boyd, S., Rashti, M.R., Esfandbod, M., Kuzyakov, Y., 2021. Soil organic matter formation is controlled by the chemistry and bioavailability of organic carbon inputs across different land uses. Sci. Total Environ. 770, 145307.
Bai, Y., Cotrufo, M.F., 2022. Grassland soil carbon sequestration: current understanding, challenges, and solutions. Science 377 (6606), 603–608.
Beckie, H.J., Jasieniuk, M., 2021. Lolium rigidum and Lolium multiflorum. In: Biology and Management of Problematic Crop Weed Species. Academic Press, pp. 261–283.
Benner, R., Hatcher, P.G., Hedges, J.I., 1990. Early diagenesis of mangrove leaves in a tropical estuary: bulk chemical characterization using solid-state 13C NMR and elemental analyses. Geochim. Cosmochim. Acta 54 (7), 2003–2013.
Blair, N.E.A.L., Leu, A., Olsen, J., Kwong, E., Des Marais, D., 1985. Carbon isotopic fractionation in heterotrophic microbial metabolism. Appl. Environ. Microbiol. 50 (4), 996–1001.
Chantigny, M.H., Angers, D.A., Kaiser, K., Kalbitz, K., 2007. In: Extraction and Characterization of Dissolved Organic Matter. CRC Press, Boca Raton, Fl, USA, pp. 617–635.
Chefetz, B., Chen, Y., Clapp, C.E., Hatcher, P.G., 2000. Characterization of organic matter in soils by thermochemolysis using tetramethylammonium hydroxide (TMAH). Soil Sci. Soc. Am. J. 64, 583–589.
Christ, M.J., David, M.B., 1996. Temperature and moisture effects on the production of dissolved organic carbon in a Spodosol. Soil Biol. Biochem. 28 (9), 1191–1199.
Collado, S., Oulego, P., Suárez-Iglesias, O., Díaz, M., 2018. Biodegradation of dissolved humic substances by fungi. Appl. Microbiol. Biotechnol. 102, 3497–3511.
Cooke, R.C., Rayner, A.D., 1984. Ecology of saprotrophic fungi (pp. xiv+-415).
Cotrufo, M.F., Wallenstein, M.D., Boot, C.M., Denef, K., Paul, E., 2013. The M icrobial E fficiency-M atrix S tabilization (MEMS) framework integrates plant litter decomposition with soil organic matter stabilization: do labile plant inputs form stable soil organic matter? Glob. Chang. Biol. 19 (4), 988–995.
Cragg, S.M., Beckham, G.T., Bruce, N.C., Bugg, T.D., Distel, D.L., Dupree, P., Etxabe, A. G., Goodell, B.S., Jellison, J., McGeehan, J.E., McQueen-Mason, S.J., Schnorr, K., Walton, P.H., Watts, J.E.M., Zimmer, M., 2015. Lignocellulose degradation mechanisms across the tree of Life. Curr. Opin. Chem. Biol. 29, 108–119.
Day, T.A., Bliss, M.S., Tomes, A.R., Ruhland, C.T., Guénon, R., 2018. Desert leaf litter decay: coupling of microbial respiration, water-soluble fractions and photodegradation. Glob. Chang. Biol. 24, 5454–5470.
Eglinton, G., Hamilton, R.J., 1967. Epicuticular leaf waxes. Science 156, 1322–1335.
Eswaran, H., Van Den Berg, E., Reich, P., 1993. Organic carbon in soils of the world. Soil Sci. Soc. Am. J. 57 (1), 192–194.
Fahey, T.J., Yavitt, J.B., Sherman, R.E., Groffman, P.M., Fisk, M.C., Maerz, J.C., 2011. Transport of carbon and nitrogen between litter and soil organic matter in a Northern Hardwood Forest. Ecosystems 14, 326–340.
Fry, B., 2006. Stable isotope ecology. Springer, New York, p. 318.
Gams, W., Bissett, J., 1998. Morphology and identification of *Trichoderma*. In: Kubicek, P., Harman, G.E. (Eds.), Trichoderma and Gliocladium. Taylor and Francis, pp. 3–34.
Gentile, L., Floudas, D., Olsson, U., Persson, P., Tunlid, A., 2024. Fungal decomposition and transformation of molecular and colloidal fractions of dissolved organic matter extracted from boreal forest soil. Soil Biol. Biochem. 195, 109473.
Ghashghaie, J., Badeck, F.W., Lanigan, G., Nogués, S., Tcherkez, G., Deléens, E., Griffiths, H., 2003. Carbon isotope fractionation during dark respiration and photorespiration in C3 plants. Phytochem. Rev. 2 (1), 145–161.
Girardin, C., Rasse, D.P., Biron, P., Ghashghaie, J., Chenu, C., 2009. A method for 13C-labeling of metabolic carbohydrates within French bean leaves (Phaseolus vulgaris L.) for decomposition studies in soils. Rapid Commun. Mass Spectrom. 23, 1792–1800.
Goñi, M.A., Nelson, B., Blanchette, R.A., Hedges, J.I., 1993. Fungal degradation of wood lignins: geochemical perspectives from CuO-derived phenolic dimers and monomers. Geochim. Cosmochim. Acta 57, 3985–4002.
Haddix, M.L., Paul, E.A., Cotrufo, M.F., 2016. Dual, differential isotope labeling shows the preferential movement of labile plant constituents into mineral-bonded soil organic matter. Glob. Chang. Biol. 22 (6), 2301–2312.
Haynes, R.J., 2005. Labile organic matter fractions as centralcomponents of the quality of agricultural soils: anoverview. Adv. Agron. 5, 221–268.
He, Z., Mao, J., Honeycutt, C.W., Ohno, T., Hunt, J.F., Cade-Menun, B.J., 2009. Characterization of plant-derived water extractable organic matter by multiple spectroscopic techniques. Biol. Fertil. Soils 45, 609–616.
Hishi, T., Hirobe, M., Tateno, R., Takeda, H., 2004. Spatial and temporal patterns of water-extractable organic carbon (WEOC) of surface mineral soil in a cool temperate forest ecosystem. Soil Biol. Biochem. 36 (11), 1731–1737.
Huang, Y., Eglinton, G., van der Hage, E.R.E., Boon, J.J., Bol, R., Ineson, P., 1998. Dissolved organic matter and its parent organic matter in grass upland soil horizons studied by analytical pyrolysis techniques. Eur. J. Soil Sc. 49, 1–15.
Humphreys, M., Feuerstein, U., Vandewalle, M., Baert, J., 2010. Ryegrasses. Boller, B., et al. (Eds.), Handbook of plant breeding: fodder crops and amenity grasses.
Jones, M.B., Donnelly, A., 2004. Carbon sequestration in temperate grassland ecosystems and the influence of management, climate and elevated CO2. New Phytol. 164 (3), 423–439.
Kalbitz, K., Geyer, W., Geyer, S., 1999. Spectroscopic properties of dissolved humic substances – a reflection of land use history in a fen area. Biogeochemistry 47, 219–238.
Kalbitz, K., Solinger, S., Park, J.H., Michalzik, B., Matzner, E., 2000. Controls on the dynamics of dissolved organic matter in soils: a review. Soil Sci. 165 (4), 277–304.
Kalbitz, K., Schwesig, D., Schmerwitz, J., Kaiser, K., Haumaier, L., Glaser, B., Leinweber, P., 2003. Changes in properties of soil-derived dissolved organic matter induced by biodegradation. Soil Biol. Biochem. 35 (8), 1129–1142.
Kelleher, B.P., Simpson, A.J., 2006. Humic substances in soils: are they really chemically distinct? Environ. Sci. Technol. 40 (15), 4605–4611.
Khatami, S., Deng, Y., Tien, M., Hatcher, P.G., 2019. Formation of water-soluble organic matter through fungal degradation of lignin. Org Geochem. 135, 64–70.
Kemmitt, S.J., Lanyon, C.V., Waite, I.S., Wen, Q., Addiscott, T.M., Bird, N.R.A., O'Donnell, A.G., Brookes, P.C., 2008. Mineralization of native soil organic matter is not regulated by the size, activity or composition of the soil microbial biomass—a new perspective. Soil Biol. Biochem. 40, 61–73.
Kéraval, B., Lehours, A.C., Colombet, J., Amblard, C., Alvarez, G., Fontaine, S., 2016. Soil carbon dioxide emissions controlled by an extracellular oxidative metabolism identifiable by its isotope signature. Biogeosciences 13, 6353–6362.
Kögel-Knabner, I., 2002. The macromolecular organic composition of plant and microbial residues as inputs to soil organic matter. Soil Biol. Biochem. 34 (2), 139–162.
Kögel-Knabner, I., 2017. The macromolecular organic composition of plant and microbial residues as inputs to soil organic matter: fourteen years on. Soil Biol. Biochem. 105, A3–A8.
Lal, R., 2008. Carbon sequestration. Philos. Trans. R. Soc., B 363 (1492), 815–830.
Lehmann, J., Kleber, M., 2015. The contentious nature of soil organic matter. Nature 528 (7580), 60–68.
Lerch, T.Z., Nunan, N., Dignac, M.F., Chenu, C., Mariotti, A., 2011. Variations in microbial isotopic fractionation during soil organic matter decomposition. Biogeochemistry 106, 5–21.
Li, T., Zhang, J., Wang, X., Hartley, I.P., Zhang, J., Zhang, Y., 2022. Fungal necromass contributes more to soil organic carbon and more sensitive to land use intensity than bacterial necromass. Appl. Soil Ecol. 176, 104492.
Liang, C., Schimel, J.P., Jastrow, J.D., 2017. The importance of anabolism in microbial control over soil carbon storage. Nat. Microbiol. 2 (8), 1–6.
Lohse, K.A., Pierson, D., Patton, N.R., Sanderman, J., Huber, D.P., Finney, B., Facer, J., Meyers, J., Seyfried, M.S., 2022. Multiscale responses and recovery of soils to wildfire in a sagebrush steppe ecosystem. Sci. Rep. 12 (1), 22438.
Maie, N., Jaffé, R., Miyoshi, T., Childers, D.L., 2006. Quantitative and qualitative aspects of dissolved organic carbon leached from senescent plants in an oligotrophic wetland. Biogeochemistry 78, 285–314.
Maire, V., Alvarez, G., Colombet, J., Comby, A., Despinasse, R., Dubreucq, E., Fontaine, S., 2013. An unknown oxidative metabolism substantially contributes to soil CO 2 emissions. Biogeosciences 10 (2), 1155–1167.
Mandels, M., Reese, E., 1957. Induction of cellulase in *Trichoderma viridae* as influenced by carbon source and metals. J. Bacteriol. 73, 269–278.
Margenot, A.J., Calderón, F.J., Parikh, S.J., 2016. Limitations and potential of spectral substractions in Fourier-transform Infrared spectroscopu of soil samples. Soil Sci. Soc. Am. J. 80, 10–26.
Medina, J., Monreal, C.M., Orellana, L., Calabi-Floody, M., González, M.E., Meier, S., Borie, F., Cornejo, P., 2020. Influence of saprophytic fungi and inorganic additives on enzyme activities and chemical properties of the biodegradation process of wheat straw for the production of organo-mineral amendments. J. Environ. Manage. 255, 109922.
Mikutta, R., Kleber, M., Torn, M.S., Jahn, R., 2006. Stabilization of soil organic matter: association with minerals or chemical recalcitrance? Biogeochemistry 77, 25–56.

Nakakuni, M., Kuwahara, V.S., Yamamoto, S., 2023. Organic compounds in aquatic sediments analyzed by pyrolysis–GC–MS with tetramethylammonium hydroxide (TMAH) and alkaline CuO oxidation methods. J. Anal. Appl. Pyrol. 172, 106016.
Nakas, J.P., Klein, D., 1979. Decomposition of microbial cell components in a semi-arid grassland soil. Appl. Environ. Microbiol. 38 (3), 454–460.
Nishimura, S., Maie, N., Baba, M., Sudo, T., Sugiura, T., Shima, E., 2012. Changes in the quality of chromophoric dissolved organic matter leached from senescent leaf litter during the early decomposition. J. Environ. Qual. 41 (3), 823–833.
Opsahl, S., Benner, R., 1995. Early diagenesis of vascular plant tissues: Lignin and cutin decomposition and biogeochemical implications. Geochim. Cosmochim. Acta 59, 4889–4904.
Osono, T., Takeda, H., 2001. Organic chemical and nutrient dynamics in decomposing beech leaf litter in relation to fungal ingrowth and succession during 3-year decomposition processes in a cool temperate deciduous forest in Japan. Ecol. Res. 16, 649–670.
Pichler, M., Kögel-Knabner, I., 2000. Chemolytic analysis of organic matter during aerobic and anaerobic treatment of municipal solid waste (Vol. 29, No. 4, pp. 1337-1344). American Society of Agronomy, Crop Science Society of America, and Soil Science Society of America.
Pouwels, A.D., Eijkel, G.B., Boon, J.J., 1989. Curie-point pyrolysis-capillary gas chromatography-high-resolution mass spectrometry of microcrystalline cellulose. J. Anal. Appl. Pyrol. 14, 237–280.
R Development Core Team R: A Language and Environment for Statistical Computing 2015.
Robertson, S.A., Mason, S.L., Hack, E., Abbott, G.D., 2008. A comparison of lignin oxidation, enzymatic activity and fungal growth during white-rot decay of wheat straw. Org Geochem. 39 (8), 945–951.
Said-Pullicino, D., Erriquens, F.G., Gigliotti, G., 2007. Changes in the chemical characteristics of water-extractable organic matter during composting and their influence on compost stability and maturity. Bioresour. Technol. 98 (9), 1822–1831.
Saiz-Jimenez, C., de Leeuw, J.W., 1986. Lignin pyrolysis products: their structures and their significance as biomarkers. Org Geochem. 10, 869–876.
Saiz-Jimenez, C., Martin-Sanchez, P.M., Gonzalez-Perez, J.A., Hermosin, B., 2021. Analytical pyrolysis of the fungal melanins from *Ochroconis* spp. isolated from lascaux cave, France. Appl. Sci. 11, 1198.
Salamanca, E.F., Kaneko, N., Katagiri, S., 2003. Rainfall manipulation effects on litter decomposition and the microbial biomass of the forest floor. Appl. Soil Ecol. 22 (3), 271–281.
Sánchez-Corzo, L.D., Álvarez-Gutiérrez, P.E., Meza-Gordillo, R., Villalobos-Maldonado, J.J., Enciso-Pinto, S., Enciso-Sáenz, S., 2021. Lignocellulolytic enzyme production from wood rot fungi collected in Chiapas, Mexico, and their growth on lignocellulosic material. Journal of Fungi 7 (6), 450.
Shen, D.K., Gu, S., 2009. The mechanism for thermal decomposition of cellulose and its main products. Bioresour. Technol. 100, 6496–6504.
Six, J., Frey, S.D., Thiet, R.K., Batten, K.M., 2006. Bacterial and fungal contributions to carbon sequestration in agroecosystems. Soil Sci. Soc. Am. J. 70 (2), 555–569.
Sharma, S., Kour, D., Rana, K.L., Dhiman, A., Thakur, S., Thakur, P., Singh, K., 2019. Trichoderma: biodiversity, ecological significances, and industrial applications. In: *Recent advancement in white biotechnology through fungi: volume 1: diversity and enzymes perspectives*. Springer International Publishing, Cham, pp. 85–120.
Sharma, V., Chauhan, R., Kumar, R., 2021. Spectral characteristics of organic soil matter: a comprehensive review. Microchem. J. 171, 106836.
Sobeih, K.L., Baron, M., Gonzalez-Rodriguez, J., 2008. Recent trends and developments in pyrolysis–gas chromatography. J. Chromatogr. A 1186 (1–2), 51–66.
Stankiewicz, B.A., van Bergen, P.F., Duncan, I.J., Carter, J.F., Briggs, D.E.G., Evershed, R. P., 1996. Recognition of chitin and proteins in invertebrate cuticles using analytical pyrolysis/gas chromatography and pyrolysis/gas chromatography/mass spectrometry. Rapid Commun. Mass Spectrom. 10, 1747–1757.
Spencer, R.G.M., Stubbins, A., Hernes, P.J., Baker, A., Mopper, K., Aufdenkampe, A.K., Dyda, R.Y., Mwamba, V.L., Mangangu, A.M., Wabakanghanzi, J.N., Six, J., 2009. Photochemical degradation of dissolved organic matter and dissolved lignin phenols from the Congo River. J. Geophys. Res. 115, G03010.
Stevenson, F.J., 1982. Humus. Chemistry: genesis, composition, reactions. John Wiley & Sons Inc., New York.
Szymanski, W., 2017. Chemistry and spectroscopic properties of surface horizons of Arctic soils under different types of tundra vegetation – a case study from the Fuglebergsletta coastal plain (SW Spitsbergen). Geoderma 305, 30–39.
Tcherkez, G., 2010. Isotopie biologique: Introduction aux effets isotopiques et à leurs applications en biologie. Lavoisiern Éd. Tec & Doc.
Templier, J., Gallois, N., Derenne, S., 2013. Analytical TMAH pyrolysis of dipeptides: formation of new complex cyclic compounds related to the presence of the peptide bond. J. Anal. Applied Pyrolysis 104, 684–694.
Tiwari, P., Misra, B.N., Sangwan, N.S., 2013. β-glucosidases from the fungus Trichoderma: an efficient cellulase machinery in biotechnological applications. Biomed Res. Int. 2013 (1), 203735.
Toosi, E.R., Doane, T.A., Horwath, W.R., 2012. Abiotic solubilization of soil organic matter, a less-seen aspect of dissolved organic matter production. Soil Biol. Biochem. 50, 12–21.
Toosi, E.R., Schmidt, J.P., Castellano, M.J., 2014. Soil temperature is an important regulatory control on dissolved organic carbon supply and uptake of soil solution nitrate. Eur. J. Soil Biol. 61, 68–71.
Urey, H.C., 1947. The thermodynamic properties of isotopic substances. J. Chem. Soc. (Resumed) 562–581.
Wang, M., Zhang, Z., Wang, Y., Mo, X., Zhang, Q., Zhang, P., Yin, G., Li, L., Wang, S., Mo, J., Zhang, W., Wang, J.J., 2021a. Characteristics of dissolved organic matter and dissolved lignin phenols in tropical forest soil solutions during rainy seasons and their responses to nitrogen deposition. ACS Earth Space Chem. 5, 3150–3158.
Wang, Q.W., Pieristè, M., Liu, C., Kenta, T., Robson, T.M., Kurokawa, H., 2021b. The contribution of photodegradation to litter decomposition in a temperate forest gap and understorey. New Phytol. 229, 2625–2636.
Zhou, X., Chen, L., Li, Y., Xu, J., Brookes, P.C., 2020. Abiotic processes dominate soil organic matter mineralization: investigating the regulatory gate hypothesis by inoculating a previously fumigated soil with increasing fresh soil inocula. Geoderma 373, 114400.
Zhu, L., Cao, M., Sang, C., Li, T., Zhang, Y., Chang, Y., Li, L., 2022a. Trichoderma bio-fertilizer decreased C mineralization in aggregates on the southern North China Plain. Agriculture 12 (7), 1001.
Zhu, J., Wu, Q., Wu, F., Yue, K., Ni, X., 2022b. Decline in carbon decomposition from litter after snow removal is driven by a delayed release of carbohydrates. Plant and Soil 481 (1), 83–95.
Ziegler, F., Kögel, I., Zech, W., 1986. Alteration of gymnosperm and angiosperm lignin during decomposition in forest humus layers. Zeitschrift Für Pflanzenernährung Und Bodenkunde 149 (3), 323–331.
Zonneveld, K.A., Versteegh, G.J., Kasten, S., Eglinton, T.I., Emeis, K.C., Huguet, C., Wakeham, S.G., 2010. Selective preservation of organic matter in marine environments; processes and impact on the sedimentary record. Biogeosciences 7 (2), 483–511.